BMC Medical Genomics

RESEARCH Open Access

Clinical characteristics and genetic analysis of four pediatric patients with Kleefstra syndrome

Rong Ren[1], Yedan Liu[2†], Peipei Liu[2†], Jing Zhao[1], Mei Hou[1], Shuo Li[3], Zongbo Chen[2] and Aiyun Yuan[1*]

Abstract

Background Kleefstra syndrome spectrum (KLEFS) is an autosomal dominant disorder that can lead to intellectual disability and autism spectrum disorders. KLEFS encompasses Kleefstra syndrome-1 (KLEFS1) and Kleefstra syndrome-2 (KLEFS2), with KLEFS1 accounting for more than 75%. However, limited information is available regarding KLEFS2. KLEFS1 is caused by a subtelomeric chromosomal abnormality resulting in either deletion at the end of the long arm of chromosome 9, which contains the *EHMT1* gene, or by variants in the *EHMT1* gene and the *KMT2C* gene that cause KLEFS2.

Methods This study was a retrospective analysis of clinical data from four patients with KLEFS. Exome sequencing (ES) and Sanger sequencing techniques were used to identify and validate the candidate variants, facilitating the analysis of genotype–phenotype correlations of the *EHMT1* and *KMT2C* genes. Protein structure modeling was performed to evaluate the effects of the variants on the protein's three-dimensional structure. In addition, real-time quantitative reverse transcription–polymerase chain reaction (RT–qPCR) and western blotting were used to examine the protein and mRNA levels of the *KMT2C gene*.

Results Two patients with KLEFS1 were identified: one with a novel variant (c.2382 + 1G > T) and the other with a previously reported variant (c.2426 C > T, p.Pro809Leu) in the *EHMT1* gene. A *De novo* deletion at the end of the long arm of chromosome 9 was also reported. Furthermore, a patient with KLEFS2 was identified with a novel variant in the *KMT2C* gene (c.568 C > T, p.Arg190Ter). The RT–qPCR and western blot results revealed that the expression of the *KMT2C* gene was downregulated in the KLEFS2 sample.

Conclusion This study contributes to the understanding of both KLEFS1 and KLEFS2 by identifying novel variants in *EHMT1* and *KMT2C* genes, thereby expanding the variant spectrum. Additionally, we provide the first evidence of how a *KMT2C* variant leads to decreased gene and protein expression, enhancing our understanding of the molecular mechanisms underlying KLEFS2. Based on these findings, children exhibiting developmental delay, hypotonia,

†Yedan Liu and Peipei Liu these authors contributed equally to this work.

*Correspondence:
Aiyun Yuan
yay79429@126.com

Full list of author information is available at the end of the article

distinctive facial features, and other neurodevelopmental abnormalities should be considered for ES to ensure early intervention and treatment.

Keywords Kleefstra syndrome-1 (KLEFS1), Kleefstra syndrome-2 (KLEFS2), *KMT2C* gene, *EHMT1* gene, Exome sequencing (ES), RT–qPCR

Introduction

Kleefstra syndrome spectrum (KLEFS) is a rare autosomal dominant disorder that was first reported by Kleefstra et al. in 2006 [1]. The typical clinical manifestations of KLEFS include intellectual disability (ID), developmental delay, autism spectrum disorder (ASD), hypotonia, and distinctive facial features. Less commonly, cardiorespiratory and renal defects, epilepsy, and psychiatric disorders may also occur [2]. KLEFS can be classified as Kleefstra syndrome-1 (KLEFS1, OMIM: 610253) or Kleefstra syndrome-2 (KLEFS2, OMIM: 617768). The etiology of KLEFS1 is currently attributed to variants in the *EHMT1* gene or to a deletion at the end of the long arm of chromosome 9 containing the *EHMT1* gene, while variants in the *KMT2C* gene cause KLEFS2. Both KLEFS1 and KLEFS2 are caused by genetic defects involving histone methyltransferases. Variants in *MBD5*, *SMARCB1*, *NR1I3*, and other genes, referred to as the KLEFS gene, can also lead to KLEFS [3].

KLEFS1 accounts for more than 75% of KLEFS cases and is characterized by a range of clinical manifestations, including ID, developmental delays, and hypotonia. Other clinical manifestations, including congenital heart disease, genital anomalies, epilepsy, hearing impairment, behavioral problems, sleep disorders, psychiatric disorders, and ASD, have also been reported [4–7]. Most patients exhibit distinctive facial features, such as microcephaly, arched eyebrows, short noses, upturned nostrils, and ectropion of the lower lip [8, 9]. Most children with KLEFS2 display a range of conditions, including ID, ASD, hypotonia, and peculiar distinctive features. However, the clinical presentation and diagnostic criteria for KLEFS2 are currently insufficient, and its long-term prognosis remains unclear [10].

Owing to the diverse and complex clinical manifestations of KLEFS, early identification, timely intervention, and comprehensive treatment and rehabilitation are particularly crucial. In this study, we present four KLEFS patients treated at the Women's and Children's Hospital of Qingdao University. Among them, three patients were diagnosed with KLEFS1, featuring an *EHMT1* splice site variant, a missense variant, and deletion at the end of the long arm of chromosome 9, includes the *EHMT1* gene. One patient was diagnosed with KLEFS2, associated with a nonsense variant in *KMT2C*. The diagnostic and treatment processes for these patients are detailed below. Additionally, a review of the relevant literature is provided to offer insights into early diagnosis, treatment strategies, and prognosis for children with KLEFS.

Materials and methods

Subjects

Four patients who displayed unexplained developmental delay and facial anomalies underwent genetic testing and ultimately diagnosed with KLEFS at the Affiliated Women and Children's Hospital of Qingdao University. Genetic tests were prompted due to the patients unexplained developmental delays and facial anomalies. All cases were assessed using the Gesell Developmental Schedules (GDS, https://gesellinstitute.org/) to determine the extent of the developmental delays. The study was approved by our hospital, with the approval number QFELL-YJ-2024-06. Informed consent was obtained from each patient after a full explanation of the study was provided.

Exome sequencing (ES) and sanger sequencing

Genomic DNA was extracted from the peripheral blood samples of patients and their parents for exome sequencing. A DNA Sample Prep Reagent Set (MyGenostics, Beijing, China) was used for the preparation of standard Illumina libraries. The gene panel for KLEFS disease was downloaded from the ClinVar database. Biotinylated capture probes were designed to cover coding exons and flanking regions. The DNA was eluted and amplified after hybridization and bead washing. The PCR product was purified and sequenced on an Illumina HiSeq X Ten sequencer for paired 150 bp reads.

After sequencing, the raw data were saved in FASTQ format. The clean reads were mapped to the UCSC hg19 human reference genome using the BWA parameter in Sentieon software (https://www.sentieon.com/). Duplicated reads were removed using the parameter driver of Sentieon software, and the base quality was corrected to more accurately reflect the probability of mismatch with the reference genome. The mapped reads were used for variant detection. SNP and InDel variants were detected using the parameter driver of Sentieon software, and the data were subsequently transformed to the VCF format. Variants were further annotated via ANNOVAR software (http://annovar.openbioinformatics.org/en/latest/) and associated with multiple databases, such as 1000 Genomes, ESP6500, dbSNP, EXAC, Inhouse (MyGenostics), and HGMD. For CNV analysis, the same preprocessing steps were followed, and CNVkit (https://cnvkit

.readthedocs.io/en/stable/) software was used to extract CNV information.

In this study, potentially pathogenic variants were selected in four steps: (i) variant reads > 5 with a ratio ≥ 30%; (ii) exclusion of variants with a frequency > 5% in 1000 g, ESP6500, and in-house databases; (iii) removal of variants in the InNormal database (MyGgnostics); and (iv) exclusion of (synonymous variants not found in the HGMD database. For variant validation and family segregation analysis, Sanger sequencing was performed. Medical laboratory geneticists classified the remaining variants according to ACMG guidelines [11].

Silico evaluation: variant model evaluation

We used NCBIGene (https://www.ncbi.nlm.nih.gov/) to obtain the *EHMT1* (NM_024757) and *KMT2C* (NM_170606.3) gene sequences and the AlphaFold protein structure database (https://AlphaFold.ebi.ac.uk/) to obtain the *EHMT1* and *KMT2C* gene protein 3D structures. The protein 3D structure visualization software PyMOL 2.5 was used to generate protein 3D structure maps.

RT–qPCR amplification

After providing informed consent, total RNA was isolated from the blood samples of Patient 4 and his parents with RNAios plus reagent (9108, TAKARA) for molecular genetic analysis. Total RNA was reverse transcribed to cDNA via the Cw2569 Reverse Transcription Kit (CWBIO, China). cDNA was amplified via real-time quantitative reverse transcription–polymerase chain reaction (RT–qPCR) to determine the expression of the *KMT2C* gene, which encodes a histone methyltransferase, in Patient 4 and his parents. The transcripts were quantified via RT–qPCR on an ABI PRISM 7300 Sequence Detector (Perkin-Elmer Applied Biosystems) with TAKARA 9108 predesigned SYBRW Premix Ex Taq™ assays and reagents (Mxbio, Shanghai, China) according to the manufacturer's instructions. The following specific primers were used for RT–qPCR: hGAPDH (5'-GCACCGTCAAGGCTGAGAAC-3') and h*KMT2C* (5'-GCCTGTTCTCAGTGTGGTCA-3'). The RT–qPCR program included ab initial denaturation at 95 °C for 5 min, followed by 40 cycles of denaturation at 95 °C for 15 s, annealing at 60 °C for 30 s, and a final extension at 60 °C for 2 min. After the reaction, amplification and melting curves were analyzed, and the 2-△△Ct value was calculated to determine the fold change in gene expression relative to that of the controls.

Western blot analysis

Protein pellets were obtained from the peripheral blood of P4 and its parents. (i) Protein quantification: The total protein concentration of the samples was determined using a BCA protein quantification kit (Beyotime, P0010), and each sample was adjusted to a concentration of 1 mg/ml. (ii) Gel casting: A 12% separating gel with a total volume of 10 ml was prepared. The gel was poured immediately and allowed to polymerize for 45 min at room temperature. A 5% stacking gel with a total volume of 5 ml was prepared and poured onto the separating gel. After polymerization, the gel was placed in the electrophoresis chamber, and electrophoresis buffer was added. (iii) Electrophoresis: Protein extraction solutions from each treatment group were mixed, adjusted to a concentration of 1 mg/ml, and mixed with an equal volume of 2× sample buffer. The samples were boiled, cooled, and centrifuged before being loaded onto the gel. Electrophoresis was performed at a constant voltage of 70 V for approximately 30 min, followed by 90 V until the bromophenol blue reached approximately 0.5 cm from the bottom of the gel. (iv) Protein transfer and immunodetection: PVDF membranes were prepared and combined with the gel to form a transfer sandwich. The transfer was performed at a constant current of 200 mA for 70 min. After transfer, the PVDF membrane was blocked with 5% BSA, washed, and incubated with primary antibodies (*KMT2C* Antibody, Proteintech 28437-1-AP, dilution: 1:500) overnight at 4 °C. After washing, the membrane was incubated with secondary antibodies, washed again, and subjected to chemiluminescence detection.

Results

Case presentation

Proband 1 (P1), a 2-year-old male, was the second full-term birth delivered through cesarean section with a birth weight of 3.6 kg from a non-consanguineous healthy couple (mother 45 years old). The patient was brought to the Affiliated Women and Children's Hospital of Qingdao University due to "developmental delay since birth." He achieved head stability at 4–5 months, rolled over at 6–7 months, and sat independently at 10–11 months. However, crawling was not observed, and active language expression was lacking until 11 months. Physical examination revealed distinctive facial features: head circumference of 44.8 cm (-1SD ~ 0SD, growth standard for children under 7 years of age, Health Industry Standards of China), yellow hair, flat forehead, hypertelorism, joint hypermobility, a depressed nasal bridge, hypodontia with wide interdental spacing, trunk and lower limb hypotonia, inability to walk, and pes planus during walking (Fig. 1). Ultrasonography of the urogenital system indicated retractile testes, and echocardiography revealed a patent foramen ovale. Audiological evaluation showed mild hearing impairment, with 35 decibels in the left ear and 30 in the right ear. Liver and kidney function tests, cranial magnetic resonance imaging (MRI),

Fig. 1 Clinical photographs of patient **A**: P1 showed a head circumference of 44.8 cm (-1 SD, growth standard for children under 7 years of age, Health Industry Standards of China), with yellow hair, flat forehead, hypertelorism, joint hypermobility, a depressed nasal bridge, and hypodontia with wide interdental spacing; **B**: P2 showed a broad forehead, hypertelorism, low and flat nasal bridge, slightly thick lips, high-arched palate, macroglossia, small teeth, and a pigmented lesion of 1.8 cm × 2 cm on the left outer side of the lower leg; **C**: P3 exhibited a depressed nasal bridge, anteverted nares and hypertelorism; **D**: P4 had a head circumference of 43 cm (-1SD~-2SD) and pectus carinatum

electrocardiogram, and electroencephalogram revealed no apparent abnormalities.

Proband 2 (P2), a 3-year-old female, was the second full-term birth delivered through cesarean section, with a birth weight of 3.4 kg from a non-consanguineous healthy couple. At 5 days postnatal, she was hospitalized for 10 days due to severe neonatal jaundice. During her hospitalization, cranial MRI revealed mild intracranial hemorrhage, but follow-up cranial MRI showed no apparent abnormalities. She was referred to our hospital because of "Delayed speech development." Her developmental milestones were significantly delayed compared to those of her peers, with independent walking achieved at 1 year and 7 months. Feeding difficulties and umbilical hernias were also observed. The ability to say "mama" was acquired at 1 year and 5 months, reflecting delayed speech development. Physical examination revealed distinctive facial features, including a broad forehead, hypertelorism, a low and flat nasal bridge, slightly thick lips, a high-arched palate, macroglossia, small teeth, and a pigmented lesion of 1.8 cm × 2 cm on the left outer side of the lower leg (Fig. 1). Hypotonia was observed in all limbs. At 10 months, the Bayley Scales of Infant Development Assessment revealed both a Psychomotor Development Index and Mental Development Index below 50, and consistent with developmental levels of approximately 7 and 6 months, respectively. At 1 year of age, cranial MRI revealed ventricular and sulcal widening. Laboratory investigations revealed a lactate level of 2.29 mmol/L (normal range: 1.33–1.78 mmol/L).

Proband 3 (P3), a 1-year-old female, was the second full-term birth delivered through cesarean section, with a birth weight of 4.25 kg from a non-consanguineous healthy couple. She was referred to our hospital for "developmental delay since birth". She was able to sit without support at 9 months of age and occasionally imitated saying "mama" at the age of 1 year, indicating delayed speech development. Feeding difficulties were also noted. On physical examination, facial anomalies include a depressed nasal bridge, anteverted nares, and hypertelorism (Fig. 1). Hypotonia was also observed. A cranial MRI, performed at 6 months, revealed bilateral widening of the frontotemporal extracerebral spaces. Moreover, echocardiography revealed a secundum atrial septal defect measuring approximately 3.1 mm in size, a patent ductus arteriosus, and mild tricuspid regurgitation. Audiological examination indicated moderate hearing impairment.

Proband 4 (P4), a 2-year-old male, was the first full-term infant born at 36^{+5} weeks, with a birth weight of 2.45 kg, to a non-consanguineous healthy couple (35-year-old mother). The patient presented to our hospital with the chief complaint of "developmental delay since birth". At 9 months of age, he exhibited instability while sitting independently, failure to crawl, delayed ability to stand, poor fine motor coordination, impaired ability to follow commands, and delayed speech development. Feeding difficulties since infancy, failure to thrive, and recurrent eczema were also observed. Physical examination revealed a head circumference of 43 cm (-1SD~-2SD), pectus carinatum, and hypotonia. (Fig. 1). Subsequent investigations revealed microcytic anemia in multiple routine blood examinations (last examination at 1 year of age: hemoglobin concentration, 94.00 g/L; mean corpuscular volume, 56.10 fL; mean corpuscular hemoglobin, 17.30 pg; and mean corpuscular hemoglobin concentration, 306.00 g/L). Elevated blood lactate levels of 2.17 mmol/L and elevated serum β-hydroxybutyrate levels of 1.79 mmol/L (normal range: 0.02–0.27 mmol/L) were noted. Urine creatinine was elevated at 6720.03 μmol/L, and urinalysis revealed proteinuria (±) with visible calcium oxalate crystals. A cranial MRI revealed microcytic anemia bilaterally in the temporal region, and a cranial CT scan confirmed the findings. Metabolic screening, along with ultrasound of hepatobiliary and urinary systems, gastrointestinal ultrasound,

Table 1 Scores of the gesell developmental scales in five patients

Patient ID	Ageatassessment (months)	Gesell Developmental Schedulesscores (DQ)				
		Gross motor	Finemotor	Adaptative-behaviors	Language	Personal-social
P1	20	74	57	57	59	64
P2	36	62	62	62	40	62
P3	15	71	77	69	59	70
P4	11	55	78	57	74	59

Note: DQ, development quotient. 100: normal; 85–99: below normal level; 75–84: close to mild defect; 55–74: mild defect; 40–54: moderate defect; 25–39: severe defect; < 25: extremely severe defect

Table 2 Genetic information of the KLEFS patients in our study

Patient ID	Gene of variant	Gender	Age (month)	Type of variant	Nucleotide change	Protein change	Exon	Inheritance
P1	*EHMT1*	Male	11	Splice site	c.2382 + 1G > T	/	Exon15	*De novo*
P2	*EHMT1*	Female	10	Missense	c.2426 C > T	Pro809Leu	Exon16	*De novo*
P3	*EHMT1*	Female	6	CNV(0.17 Mb)	9q34.3 140,562,016–140,730.115 loss	/	Exon2-25	*De novo*
P4	*KMT2C*	Male	11	Nonsense	c.568 C > T	Arg190Ter	Exon4	*De novo*

Note: CNV, copy number variation

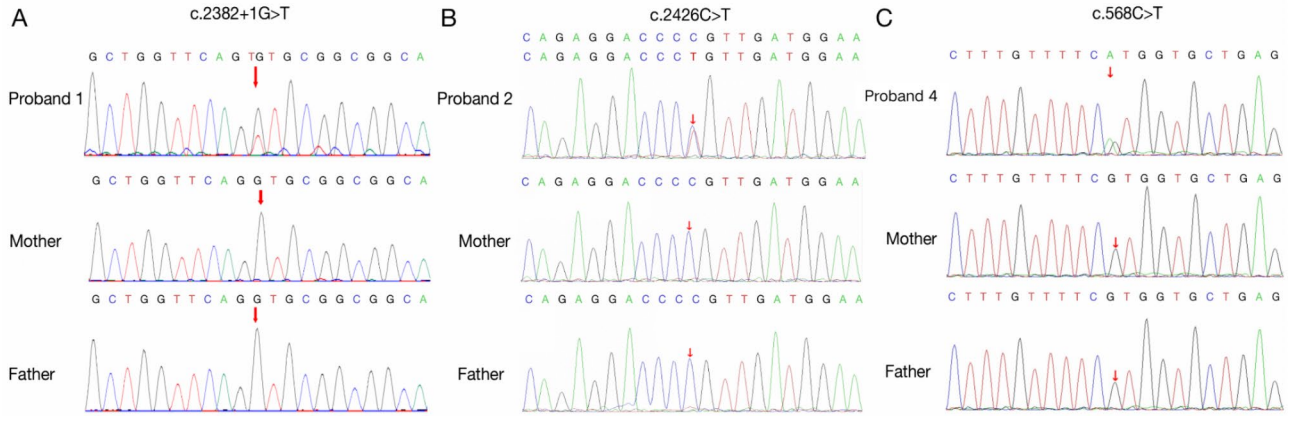

Fig. 2 DNA sequence chromatograms of the *EHMT1* and *KMT2C* variants. The arrows indicate the positions of the variants. **A**: A *De novo* variant, c.2382 + 1G > T (NM_024757.4), was found in the P1. **B**: A *De novo* variant, c.2426 C > T (p.Pro809Leu) (NM_024757), was found in the P2. **C**: A *De novo* variant, c.568 C > T (p.Arg190Ter) (NM_170606.3), was found in P4. Validation and parental origin analysis via Sanger sequencing or genetic high-throughput sequencing verified that the probands all carried *De novo* heterozygous variants

echocardiography, and electroencephalography revealed no significant abnormalities.

All these patients were subjected to GDS to assess their development. The GDS scores are listed in Table 1. The scores indicated that four patients had mild or moderate developmental delays, with notably lower scores in language development compared to other areas. Additionally, none of the patients had a family history of developmental delay or other disorders. The clinical facial features of the patients are shown in Fig. 1.

WES and sanger sequencing results

WES for P1 and P2 revealed variants in the *EHMT1* gene. For P1: NM_024757.4, c.2382 + 1G > T, the GRCh37/hg19 position (chr9:140676850) indicates a splice site variant resulting in the loss of exon 15 due to aberrant splicing. For P2: NM_024757; exon 16, c.2426 C > T (p.Pro809Leu), at position (chr9:140685343), this indicates a heterozygous missense variant. P3 exhibited a 0.17 Mb deletion of chromosome 9q34.3 (140,562,016–140,730.115)x1. This deletion region harbors the *EHMT1* gene, resulting in the loss of exon 2 to exon 25. For P4, WES revealed a variant in the *KMT2C* gene, NM_170606.3: exon4, c.568 C > T (p.Arg190Ter), at position (chr7:152012245), indicating a heterozygous nonsense variant (Table 2). Validation and parental origin analysis were performed using Sanger sequencing or high-throughput gene sequencing, confirming that the probands carried *De novo* heterozygous variants (Fig. 2). These variants were classified as pathogenic based on the variant classification guidelines of the American College of Medical Genetics and Genomics (ACMG).

Protein structural modeling

To elucidate the underlying molecular mechanism of the detected point variant, a protein modeling study was conducted. Protein modeling revealed that the c.2426 C>T variant in EHTM1 results in altered hydrogen bonding and may affect the steric structure of the protein. Originally, residue PRO809 formed a hydrogen bond with residues GLU812 and ALA813. When proline of residue PRO809 was replaced by a leucine, the hydrogen bond with residue ALA813 remained, but the hydrogen bond formed with GLU812 was lost. Moreover, the p.Arg190Ter variant in KTM2C leads directly to the loss of protein structure (including the α-helix, β-fold, and loop regions) starting from amino acid position 190 (Fig. 3).

RT–qPCR amplification results

To further validate the pathogenic molecular process caused by the newly identified variant c.568 C>T (p.Arg190Ter) in the *KMT2C* gene, we performed RNA analyses, as shown in Fig. 4. The results suggest that the child with P4 has significantly lower *KMT2C* gene expression compared to their parents, suggesting that a nonsense heterozygous variant at this locus in c.568 C>T (p.Arg190Ter) can lead to decreased expression of this gene.

Western blot analysis results

We performed western blotting (WB) using peripheral blood cells from P4 and his parents to compare possible changes in histone methyltransferase protein expression. WB analysis of whole-cell protein lysates revealed the expression of histone methyltransferases in the control group, while the protein expression signal was significantly reduced at P4 (Fig. 5). Therefore, the nonsense variant c.568 C>T (p.Arg190Ter) in the *KMT2C* gene may lead to a decrease in histone methyltransferase expression, potentially contributing to developmental delay.

Discussion

Although KLEFS1 cases have been widely reported, few KLEFS2 cases have been reported, leaving its clinical and molecular landscape less understood. Here, we report three patients with KLEFS1 variants and one patient with a KLEFS2 variant. All patients exhibited developmental delays ranging from mild to severe. Our findings highlight the critical role of gene expression regulation in neurodevelopment, particularly through the loss of function caused by *KMT2C* variants at both the RNA and protein levels.

In terms of clinical manifestations, KLEFS1 is characterized by a variety of features, including ID, ASD, developmental delay, hypotonia, and distinctive facial characteristics. Other reported phenotypes include congenital heart disease, genital anomalies, epilepsy, hearing loss, behavioral problems, sleep disorders, and psychiatric disorders. The distinctive facial features may include microcephaly, flat forehead, synophrys, hypertelorism, low nasal bridge, everted lower lip, and prognathism [4–8]. Developmental delay, particularly in language development, was commonly observed in KLEFS1. In our study, the language development of all KLEFS1 patients (the P1, the P2, and P3) significantly lagged behind that of other peers. Previous studies suggested that language developmental delays in KLEFS1 patients may be attributed to hearing impairment in the P3. However, in the P2, where no hearing impairment was evident, this observation suggests that language deficits may be an intrinsic characteristic of KLEFS1 rather than a consequence of hearing loss [12, 13]. Congenital heart diseases, including tetralogy of Fallot, incomplete development of aortic arch hypoplasia, aortic stenosis, mitral valve stenosis, pulmonary artery stenosis, pulmonary hypertension, and atrial or ventricular septal defects, have been reported in KLEFS1 patients. Additionally, cases of ventricular systolic dysfunction and dilated cardiomyopathy have been documented. Although there is considerable individual variation, cardiac disorders are considered part of the phenotype of KLEFS1 [7, 14, 15]. In this study (P1 and P2), both patients also developed congenital heart disease. Moreover, some studies have reported dental abnormalities in KLEFS1, such as hypodontia or small teeth, as observed in P1 and P2, suggesting that dental abnormalities may be characteristic features of KLEFS1 [12, 13]. Scoliosis has been reported in two KLEFS1 patients in previous studies; although these features were not observed in our patients, vigilance is necessary, as spinal scoliosis may develop with growth [16, 17]. Finally, KLEFS has been associated with obesity. While not all individuals with KLEFS develop obesity, some case studies and reviews have indicated a potential link between KLEFS and excessive weight gain. Although all of our cases presented signs of obesity, further investigation into fat metabolism could help elucidate whether there is an underlying mechanism of dysregulated fat metabolism in KLEFS [18].

At present, there are few reported cases of KLEFS2. To better study their clinical manifestations, we included 17 KLEFS2 patients aged 8 months to 31 years, including 9 males (9/17). Almost all patients exhibited varying degrees of developmental delay (14/17), ID (13/17), ASD (11/17), hypotonia (4/17), attention deficit–hyperactivity disorder (ADHD) (5/17), anemia (4/17), and epilepsy (3/17). Some patients also experienced feeding difficulties, eczema, hearing loss, sleep disorders, scoliosis, recurrent respiratory infections, microcephaly, etc. The majority of patients had distinctive facial features (10/17),

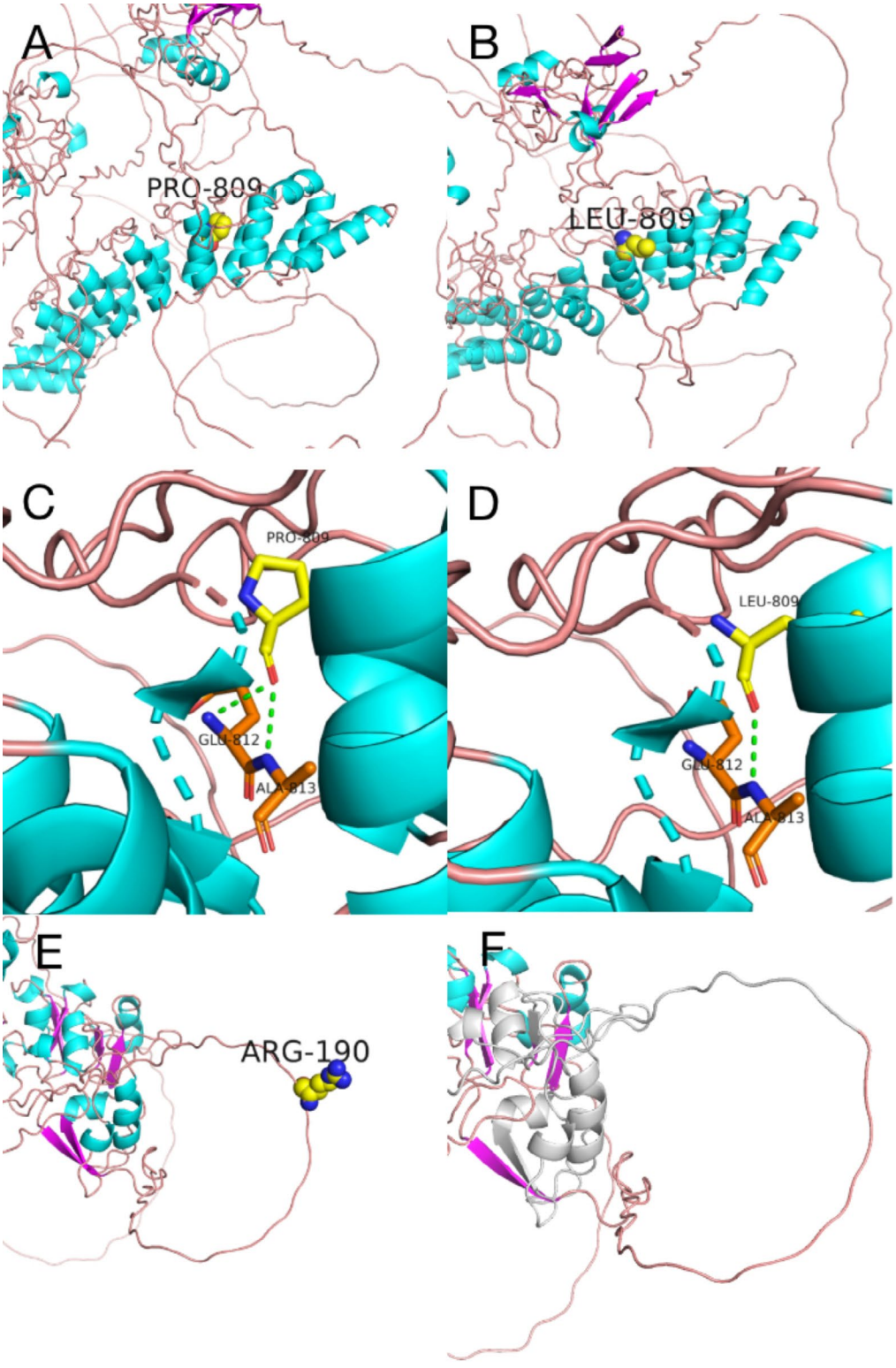

Fig. 3 Structural analysis of wild-type (WT, **A**, and **C**) and variant *EHMT1* with variants (**B** and **D**). The residues at the missense variant sites, along with the nearby functional sites, are illustrated for both WT and variant *EHMT1* via PyMol 2.5. The computed hydrogen bonds are shown as green dashed lines. P1: As shown in **A**-**D**, protein modeling revealed that the P809L variant resulted in an alteration in the number of hydrogen bonds charged from two to one. P4: Figures **E**-**F** demonstrate the p.Arg190Ter variant in the *KMT2C* gene, which results in the loss of protein structures (including α-helices, β-folds, and loop regions) starting from amino acid 190 onward, with the lost regions marked in gray

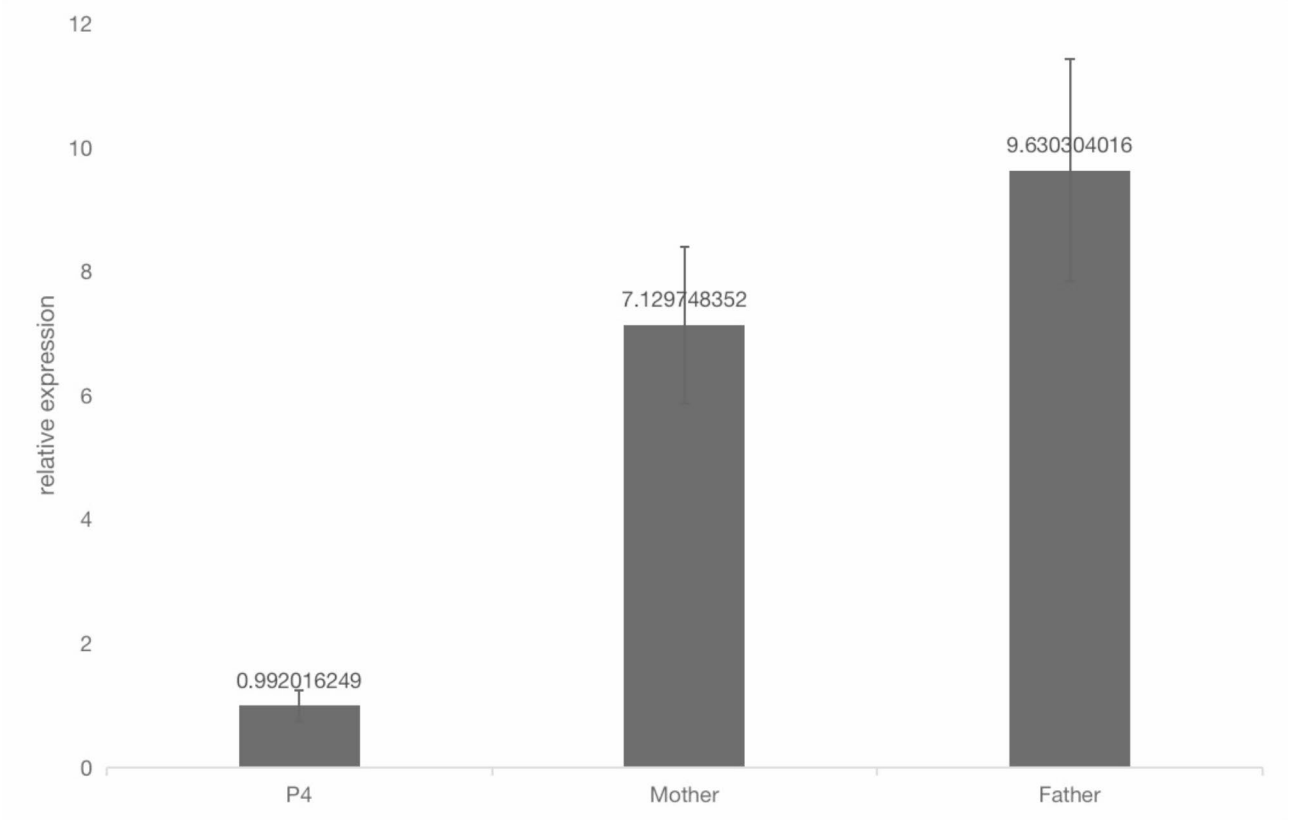

Fig. 4 *KMT2C* gene expression levels in different samples. The expression of the *KMT2C* gene in P4 was significantly lower than that in the parental samples

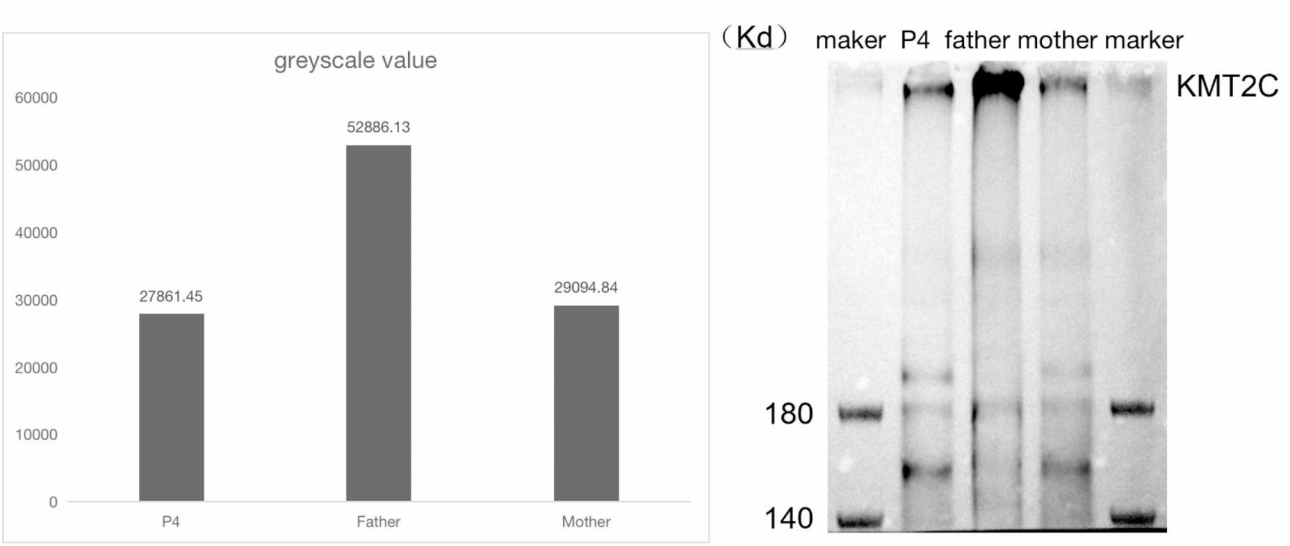

Fig. 5 WB results revealed that P4 histone methyltransferase protein expression was significantly lower than that of its parental signals

with 3 out of 5 showing abnormalities on cranial MRI, and only 1 with abnormal electroencephalogram (EEG) findings. *KMT2C* has been confirmed as a pathogenic gene for ASD (Table 3). Wu et al. [19] reported an ID patient with severe feeding difficulties and malnutrition since childhood, suggesting these may be early clinical features of the disorder. The patient's intellectual ability improved with long-term rehabilitation, indicating that such treatment could benefit KLEFS2 patients, (further studies are needed to confirm this finding. Cheema et al.

Table 3 Clinical and genetic characteristics of affected individuals with *KMT2C* variants

Ref	Gender, Age at Evaluation	Clinical characteristics						Other clinical characteristics	Unusual facies	MRI	KMT2C variants	Protein change
		ID	DD	Hypotonia	ADHD	ASD	Anemia					
[10]	Female, 6y	+	+	+	+	+	+	Aggressiveness	Macrocephalic facies, broad and rounded forehead, hypertelorism, nose with a saddle bridge and bulbous tip, ligamentous hyperlaxity, and a café au lait spot on the left thigh	Minimal gliotic changes in bilateral occipital periventricular white matter	c.9244 C > T	p.Pro3082Ser
[19]	Male, 9 m	-	+	-	+	+	+	Eczema, Feeding difficulty	Bushy brows, mandibular retrusion, and ear eczema	/	c.9284delC	p.Pro3095Lfs*2
[22]	Male, 29y	+	+	-	-	+	-	Epilepsy, Scoliosis, Phenylketonuria, Recurrent respiratory infections	Flattened midface, prominent eyebrows, thick ear helices	/	c.5216del	p.Pro1739Leufs2
	Male, 31y	+	+	-	-	+	-	Scoliosis, Strabismus, Cryptorchidism	/	/	c.7550 C > G	p.Ser2517
	Male, 15y	+	+	+	+	+	-	Bilateral inguinal hernia	Prominent eyebrows, thick ear helices	Normal	c.1690 A > T	p.Lys564
	Female, 7y	+	+		-	+	-	Sleeping disorder, Recurrent respiratory infections, Dry skin, Hoarse voice	Flattened midface, everted lower lip	Normal	c.10812_10815del	p.lys3605fs
	Female, 10y	+	+	+	+	-	-	Epilepsy, Scoliosis, Plagiocephaly	/	Nonprogressive enlarged extracerebral space	Chr7: 151,858,920–152,062,163 *De novo* deletion	/
	Female, 15y	+	+	+	-	-	-	Hyperactivity, Aggressiveness	/	/	c.4441 C > T	Arg1481*
[20]	Male, 8 m	-	+	-	-	-	-	Epilepsy, Short-statured, Microcephalic,	Bypertelorism, brachycephaly, midface hypoplasia, everted lower lip and head-tilt to the left side	Thinning of corpus callosum	c.7247_7258del	His2416_Pro2419del
[33]	Male, 3y	+	+	-	-	+	-	Sensory sensitivity, Feeding difficulty, Hyperactivity, Restlessness	Flattened midface, prominent eyebrows, a high pal-ate, a short nose, and downslanting palpebral fissures.	/	t(3;7) (q26.2;q36.1)	Exon 37
[34]	Male, 15y	-	-	-	+	+	+	Restlessness	/	/	c.12898T > C	p.Ser4300Pro
	Male, 14y	+	-	-	-	+	-	Sightly coarse facies, Dysphagia	/	/		
	Male, 8y	-	-	-	-	+	+	Dysphagia, Astigmatism	/	/		
[35]	Female, 6y2m	+	+	-	-	-	-	Macrocephaly	Mild dysmorphic	/	deletion arr[hg19] 7q36.1 (151,839,151–151,965,981)×1	/

Table 3 (continued)

Ref	Gender, Age at Evaluation	Clinical characteristics						Other clinical characteristics	Unusual facies	MRI	KMT2C variants	Protein change
		ID	DD	Hypotonia	ADHD	ASD	Anemia					
[32]	Female, 17y	+	+	-	-	-	-	Hearing loss	Marked infra-orbital creases, downslanting palpebral fissures, a duplicated right thumb.	/	c.4744G > T	p.Gly1582*
	Female, 4y	+	+	-	-	-	-	Hydrocephalus, Hypoplasia of cerebellar vermis	Marked plagiocephaly and bilateral marked bulging just below the temporal region	/	c.8849_8850delAT	p.His2950Argfs*17
	Female, 5y	+	+	-	-	+	-	Insensitivity to pain, Abnormal gait, Constipation	/	/	c.14526dupG	p.Pro4843Alafs*12

Note: ID, intellectual disability; DD, developmental delays; ADHD, attention deficit–hyperactivity disorder; ASD, autism spectrum disorder

[20] reported a KLEFS2 patient with refractory epilepsy, although this symptom was not observed in P4. Additionally, KLEFS2 patients may experience severe ADHD and ASD, which are resistant to medication and significantly impair daily life, highlighting the need for long-term behavioral interventions. In our study, P4 presented with recurrent hypopigmented microcytic anemia, a previously unreported phenotype in KLEFS2, indicating that anemia might be a clinical phenotype of KLEFS2. To our knowledge, the c.568 C > T variant of *KMT2C* reported in this study has not been previously documented. Research on *KMT2C* has been limited, with no investigations into the pathogenicity of *KMT2C* gene variants at the molecular and protein expression levels. Through protein structure prediction, RT–qPCR, and WB experiments, we demonstrated that this variant can lead to structural alterations in the protein, resulting in reduced *KMT2C* gene transcription and ultimately diminished protein expression levels. This may explain the developmental delay in patients with KLEFS2.

Based on previous studies, some KLEFS patients may also experience hearing loss. Some studies have suggested that KLEFS patients may have sensorineural or conductive neurogenic deafness [16, 20]. Psychiatric symptoms, including aggressive behavior or schizophrenia, have also been reported in KLEFS1 and KLEFS2 [2, 21]. Therefore, all confirmed KLEFS patients should undergo early assessment for psychiatric symptoms. Parents of KLEFS patients often feel concerned with anxiety, highlighting the need for healthcare professionals to provide comprehensive disease education and rehabilitation guidance. Managing KLEFS is a long-term, challenging process that demands sustained support from both families and society [12].

A substantial body of evidence confirms that variants in KLEFS genes such as *EHMT1*, *MLL3*, *SMARCB1*, *MBD5 or NR1I3* can lead to KLEFS. *EHMT1* and *MLL3* are histone modifiers. *EHMT1* catalyzes the methylation of H3K9me2 and H3K9me3, whereas *MLL3* methylates H3K4, both of which influence chromatin modification and gene expression. *SMARCB1* is part of an ATP-dependent chromatin remodeling complex, *MBD5* binds to heterochromatin, and *NR1I3* is a nuclear hormone receptor. Studies in Drosophila have revealed synergistic and antagonistic relationships between these genes, collectively regulating chromatin [22]. Frega et al. [3] reported that these KLEFS genes cause common alterations in neuronal communication, synaptic function, and neuronal excitability, offering insights into the shared mechanisms underlying ID and ASD. This finding explains the clinical homogeneity of KLEFS patients despite having different genetic variants.

Both the *EHMT1* (KLEFS1) and *KMT2C* (KLEFS2) genes are histone methyltransferases, with *EHMT1*

catalyzing H3K9 methylation and *KMT2C* targeting H3K4, both of which are crucial for regulating gene expression during neurodevelopment. For KLEFS1, we explored the pathogenic mechanisms associated with the *EHMT1* gene. The *EHMT1* gene is located at the end of the long arm of chromosome 9 and encodes euchromatic histone methyltransferase 1. KLEFS1 is primarily caused by *EHMT1* haploinsufficiency, with most cases arising from *De novo* variants and fewer being maternally inherited [23]. At the molecular and cell levels, *EHMT1* haploinsufficiency disrupts neuronal gene regulation via miRNA-mediated NRSF/REST modulation, impairs neural networks by altering their duration and frequency, affects cell cycle regulation, and impacts the morphology and distribution of subcellular structures such as the Golgi apparatus and lysosomes [24–26]. In animal studies, *EHMT1* knockout mice displayed aggressive behavior, anxiety, and ASD-like traits [27–29]. In our study, P2 shared the *EHMT1* (p.P809L) variant, presenting with ID, ASD, developmental delay, and distinct craniofacial dysmorphisms, including midface underdevelopment, consistent with previously reported cases [30]. Computational models (FoldX, molecular dynamics simulations) indicate that this variant destabilizes the *EHMT1* protein, affecting its structural integrity [31].

For KLEFS2, research on the *KMT2C* gene is rare. This gene is a crucial epigenetic regulator located on chromosome 7q36. It methylates lysine 4 of histone H3 (H3K4me1), leading to the transcription activation, participating in chromatin organization, and influencing the epigenetic regulation of brain gene expression [31]. Haploinsufficiency of *KMT2C* is often associated with developmental delay [32]. Studies in fruit flies revealed that the neurobiological mechanisms of *KMT2C* and *EHMT1* variants overlap, as both genes encode histone methyltransferases and share convergent functions in neuronal development and regulation, particularly in learning and memory [20].

Conclusions

In this study, we reported four novel patients with KLEFS, with three KLEFS1 patients exhibiting core features such as developmental delay, ID, muscle hypotonia, and distinctive facial characteristics. One of the KLEFS1 patients carried a novel pathogenic variant, c.2382+1G>T, and one had a novel *De novo* 0.17 Mb chromosome deletion at the end of the long arm of chromosome 9, which had not been reported in previous studies. Additionally, the KLEFS2 patient developed developmental delay, ID, hypotonia, anemia, recurrent eczema, and distinctive facial characteristics, harbored a novel pathogenic variant, c.568 C>T. Early ES is crucial for timely diagnosis and intervention. By identifying three novel variants, this study broadens the known KLEFS variant spectrum and opens new paths for further research into its molecular mechanisms.

Acknowledgements
The authors thank this family for contributing their help to this study.

Author contributions
Conceptualization, R.R. and A.Y.; methodology, S.L., R.R. and A.Y.; software, S.L.; validation, S.L.; formal analysis, Z.C.; investigation, J.Z.; resources, A.Y. and M.H.; data curation, P.L.; writ-ing—original draft preparation, R.R.; writing—review and editing, Y.L.; visualization, R.R. and Y.L.; supervision, Z.C.; project administration, A.Y.; funding acquisition, A.Y. All authors have read and agreed to the published version of the manuscript.

Funding
This work was supported by the Project for the Construction of the Qingdao Regional Maternal and Child Health Services Consortium.

Data availability
The datasets generated and analyzed during the current study are available in the NCBI SRA database repository (https://dataview.ncbi.nlm.nih.gov/object/PRJNA1115926?reviewer=ndgo3l3qa9chdi00s71qpepvml). ClinVar database (https://www.ncbi.nlm.nih.gov/clinvar/) [SCV005201078; SCV005205816; SCV005205815; SCV005205824].

Declarations

Ethics approval and consent to participate
The study was conducted in accordance with the Declaration of Helsinki and approved by the Institutional Review Board (or Ethics Committee) of the Affiliated Women's and Children's Hospital of Qingdao University (QFELL-YJ-2024-06).

Consent for publication
Informed consent was obtained from parents who consented to publish the images as well as the medical information supplied in this research.

Competing interests
The authors declare no competing interests.

Author details
[1]Department of Neurorehabilitation, Affiliated Women's and Children's Hospital of Qingdao University, No. 6 Tongfu Road, Qingdao 266000, Shandong, China
[2]Department of Pediatrics, Affiliated Hospital of Qingdao University, No. 16 Jiangsu Road, Qingdao 266000, Shandong, China
[3]Department of Medical Genetics, Affiliated Women's and Children's Hospital of Qingdao University, No. 6 Tongfu Road, Qingdao 266000, Shandong, China

Received: 12 May 2024 / Accepted: 11 December 2024
Published online: 18 December 2024

References

1. Kleefstra T, Brunner HG, Amiel J, Oudakker AR, Nillesen WM, Magee A, et al. Loss-of-function mutations in euchromatin histone methyl transferase 1 (EHMT1) cause the 9q34 subtelomeric deletion syndrome. Am J Hum Genet. 2006;79(2):370–7.
2. Chen CH, Huang A, Huang YS, Fang TH. Identification of a Rare Novel KMT2C variant That Presents with Schizophrenia in a Multiplex Family. J Pers Med. 2021;11(12):1254.
3. Frega M, Selten M, Mossink B, Keller JM, Linda K, Moerschen R, et al. Distinct Pathogenic Genes Causing Intellectual Disability and Autism Exhibit a Common Neuronal Network Hyperactivity Phenotype. Cell Rep. 2020;30(1):173–e1866.
4. Guterman S, Hervé B, Rivière J, Fauvert D, Clement P, Vialard F. First prenatal diagnosis of a 'pure' 9q34.3 deletion (Kleefstra syndrome): A case report and

literature review: Prenatal diagnosis of Kleefstra syndrome. J Obstet Gynaecol Res. 2018;44(3):570–5.
5. De Taevernier C, Meunier-Cussac S, Madigand J. First episode of psychosis in Kleefstra syndrome: a case report. Neurocase. 2021;27(3):227–30.
6. Torga AP, Hodax J, Mori M, Schwab J, Quintos JB. Hypogonadotropic hypogonadism and Kleefstra Syndrome due to a pathogenic variant in the EHMT1 gene: an underrecognized association. Case Rep Endocrinol. 2018;2018:4283267.
7. Okur V, Nees S, Chung WK, Krishnan U. Pulmonary hypertension in patients with 9q34.3 microdeletion-associated Kleefstra syndrome. Am J Med Genet A. 2018;176(8):1773–7.
8. Huang Q, Xiong H, Tao Z, Yue F, Xiao N. Clinical phenotypes and molecular findings in ten Chinese patients with Kleefstra Syndrome Type 1 due to EHMT1 defects. Eur J Med Genet. 2021;64(9):104289.
9. Aydin H, Bucak IH, Bagis H. Kleefstra Syndrome. J Coll Physicians Surg Pak. 2022;32(4):S76–8.
10. Siano MA, De Maggio I, Petillo R, Cocciadiferro D, Agolini E, Majolo M, et al. *De novo* variant in KMT2C Manifesting as Kleefstra Syndrome 2: Case Report and Literature Review. Pediatr Rep. 2022;14(1):131–9.
11. Richards S, Aziz N, Bale S, Bick D, Das S, Gastier-Foster J, ACMG Laboratory Quality Assurance Committee, et al. Standards and guidelines for the interpretation of sequence variants: a joint consensus recommendation of the American College of Medical Genetics and Genomics and the Association for Molecular Pathology. Genet Med. 2015;17(5):405–24.
12. Haseley A, Wallis K, DeBrosse S. Kleefstra syndrome: Impact on parents. Disabil Health J. 2021;14(2):101018.
13. Ciaccio C, Scuvera G, Tucci A, Gentilin B, Baccarin M, Marchisio P, et al. New Insights into Kleefstra Syndrome: Report of Two Novel Cases with Previously Unreported Features and Literature Review. Cytogenet Genome Res. 2018;156(3):127–33.
14. Jobic F, Lacot-Leriche E, Piton A, Le Moing AG, Mathieu-Dramard M, Costantini S, et al. Kleefstra syndrome: Recurrence in siblings due to a paternal mosaic variant. Am J Med Genet Part A. 2021;185(12):3877–83.
15. Kohli U. Shone's complex in a patient with chromosome 9q34.3 deletion (Kleefstra syndrome). Cardiol Young. 2019;29(2):249–51.
16. Okayasu T, Quesnel AM, Reinshagen KL, Nadol JB. Otopathology in Kleefstra Syndrome: A Case Report. Laryngoscope. 2020;130(8):2028–33.
17. Bonati MT, Castronovo C, Sironi A, Zimbalatti D, Bestetti I, Crippa M, et al. 9q34. 3 microduplications lead to neurodevelopmental disorders through EHMT1 overexpression. neurogenetics. 2019;20:145–54.
18. Kleefstra T, Kramer JM, Neveling K, Willemsen MH, Koemans TS, Vissers LE, et al. Disruption of an EHMT1-associated chromatin-modification module causes intellectual disability. Am J Hum Genet. 2012;91(1):73–82.
19. Wu D, Li R. Case Report: Long-Term Treatment and Follow-Up of Kleefstra Syndrome-2. Front Pediatr. 2022;10:881838.
20. Cheema HA, Waheed N, Saeed A. Kleefstra Syndrome with Severe Sensory Neural Deafness and *De novo* Novel Mutation. J Coll Physicians Surg Pak. 2022;32(2):236–8.
21. Colijn MA, Lakusta CM, Marcadier JL. Psychosis and autism without functional regression in a patient with Kleefstra syndrome. Psychiatr Genet. 2023;33(1):34–6.
22. Koemans TS, Kleefstra T, Chubak MC, Stone MH, Reijnders MRF, de Munnik S et al. DR FitzPatrick editor 2017 Functional convergence of histone methyltransferases EHMT1 and KMT2C involved in intellectual disability and autism spectrum disorder. PLoS Genet 13 10 e1006864.
23. Fear VS, Forbes CA, Anderson D, Rauschert S, Syn G, Shaw N, et al. Functional validation of variants of unknown significance using CRISPR gene editing and transcriptomics: A Kleefstra syndrome case study. Gene. 2022;821:146287.
24. Alsaqati M, Davis BA, Wood J, Jones MM, Jones L, Westwood A, et al. NRSF/REST lies at the intersection between epigenetic regulation, miRNA-mediated gene control and neurodevelopmental pathways associated with Intellectual disability (ID) and Schizophrenia. Translational Psychiatry. 2022;12(1):438.
25. Frega M, Linda K, Keller JM, Gümüş-Akay G, Mossink B, van Rhijn JR, et al. Neuronal network dysfunction in a model for Kleefstra syndrome mediated by enhanced NMDAR signaling. Nat Commun. 2019;10(1):4928.
26. Iglesias-Ortega L, Megías-Fernández C, Domínguez-Giménez P, Jimeno-González S, Rivero S. Cell consequences of loss of function of the epigenetic factor EHMT1. Cell Signal. 2023;108:110734.
27. Zheng Y, Liu A, Wang ZJ, Cao Q, Wang W, Lin L, et al. Inhibition of EHMT1/2 rescues synaptic and cognitive functions for Alzheimer's disease. Brain. 2019;142(3):787–807.
28. Wang ZJ, Zhong P, Ma K, Seo JS, Yang F, Hu Z, et al. Amelioration of autism-like social deficits by targeting histone methyltransferases EHMT1/2 in Shank3-deficient mice. Mol Psychiatry. 2020;25(10):2517–33.
29. Alonso A, Samanta A, van der Meij J, van den Brand L, Negwer M, Navarro Lobato I, et al. Defensive and offensive behaviours in a Kleefstra syndrome mouse model. Anim Cogn. 2023;26(4):1131–40.
30. Blackburn PR, Tischer A, Zimmermann MT, Kemppainen JL, Sastry S, Johnson AE, et al. A novel Kleefstra syndrome-associated variant that affects the conserved TPLX motif within the Ankyrin repeat of EHMT1 leads to abnormal protein folding. J Biol Chem. 2017;292(9):3866–76.
31. Lavery WJ, Barski A, Wiley S, Schorry EK, Lindsley AW. KMT2C/D COMPASS complex-associated diseases [KCDCOM-ADs]: an emerging class of congenital regulopathies. Clin Epigenetics. 2020;12(1):10.
32. Faundes V, Newman WG, Bernardini L, Canham N, Clayton-Smith J, Dallapiccola B, et al. Histone Lysine Methylases and Demethylases in the Landscape of Human Developmental Disorders. Am J Hum Genet. 2018;102(1):175–87.
33. Yamada M, Suzuki H, Miya F, Kosugiyama K, Ujiie T, Tonoki H, et al. Precise definition of the breakpoints of an apparently balanced translocation between chromosome 3q26 and chromosome 7q36: Role of KMT2C disruption. Congenit Anom (Kyoto). 2023;63(4):121–4.
34. Dhaliwal J, Qiao Y, Calli K, Martell S, Race S, Chijiwa C, et al. Contribution of Multiple Inherited Variants to Autism Spectrum Disorder (ASD) in a Family with 3 Affected Siblings. Genes (Basel). 2021;12(7):1053.
35. Schoch K, Tan QKG, Stong N, Deak KL, McConkie-Rosell A, McDonald MT, et al. Alternative transcripts in variant interpretation: the potential for missed diagnoses and misdiagnoses. Genet Med. 2020;22(7):1269–75.

Publisher's note